DIRECT NUMERICAL SIMULATION OF TS-WAVES BEHIND A GENERIC STEP OF A LAMINAR PROFILE IN THE DNW-NWB WIND TUNNEL

Heinrich Lüdeke[(1)], **Kai Backhaus**[(2)]

[(1)] *German Aerospace Center, Institute of Aerodynamics and Flow Technology, Lilienthalplatz 7, D-38108 Braunschweig, Heinrich.Luedeke@dlr.de*

[(2)] *Technical University Braunschweig, Institute of Fluid Mechanics, Hermann Blenk Str. 37, D-38108 Braunschweig, Backhaus.Kai@gmail.com*

KEYWORDS: DNS, ATLATUS, surface imperfection, laminar wing, TS-wave

ABSTRACT

The aim of this work is the DNS of local instabilities behind the step of a laminar airfoil. As a reference-configuration the laminar airfoil of the "ProWinGS" Project was chosen, as investigated in the DNW-NWB wind tunnel. The character of the dominating Tollmien-Schlichting (TS) waves on this profile allows 2D simulations of the flow-field by using a well-validated high-order numerical approach (see [2]), which will be sufficient for a detailed simulation of transitional modes in the region of interest.

All calculations were carried out on the original airfoil-geometry by using an entirely meshed step-geometry of the wind tunnel model. An extraction of the critical area allowed efficient time-accurate simulations of the instabilities near the step. For the extracted boundary-layer, unsteady perturbations were added at inflow, which resemble TS-modes in the step-region. Determining growth rates of these modes allow comparison with LST and the prediction of the laminar-turbulent transition. The middle part of the profile nose in the open test-section of the DNW-NWB contains an adjustable inset to allow settings of different forward and backward facing steps.

1. INTRODUCTION

Design criteria of commercial aircraft are mainly oriented by economical and ecological aspects and in particular the necessity to reduce fuel consumption. The efficiency of such an aircraft can be improved by a reduction of the total aerodynamic drag. For a common wing-profile under subsonic conditions, the friction-drag is the dominant part in the drag budget and its reduction will result in distinct savings. The friction drag of the laminar Boundary-Layer (BL) is generally lower in the subsonic flight regime in comparison with a turbulent BL. In general, such an airfoil exhibits laminar BL-profiles in the beginning, before the transition to the turbulent state appears. Consequently, an effective approach for drag-reduction is the application of laminar wings or the application of laminarization by suction or blowing [3, 4].

For present technical applications transition prediction in laminar boundary-layers is mainly carried out by local and non-local Linear Stability Theory (LST) since alternatives like Direct Numerical Simulation (DNS) of complete configurations are computationally too expensive for realistic Reynolds numbers. Though proven as a reliable tool for aircraft design, LST techniques are restricted in different ways, for example their restricted applicability for separated

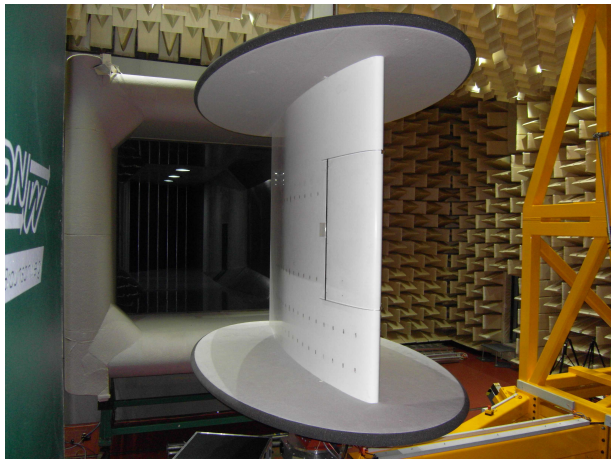

Figure 1: Investigated laminar-profile in the open DNW-NWB section

boundary-layers due to the parallel flow approach. A physics-based simulation technique would consequently provide insight into the transition scenario in such complex flow-fields and furthermore allow a verification of given LST methods, including empirical corrections for geometry-imperfections.

For this purpose, numerical studies of different accuracy and effort are possible, starting from stability calculations coupled with standard CFD simulations of entire configurations as well as basic studies of local boundary-layer flow by DNS. All these techniques have to be verified by analytical solutions and validated by experimental data from literature.

Tollmien-Schlichting (TS) waves are well known as primary instabilities in the transition process of boundary-layers from laminar to turbulent flow (Tollmien [5], Schlichting [6]). Since these modes are essentially two-dimensional instabilities their properties can be described by time accurate two-dimensional simulations, resolving the perturbation flow. For this purpose a 4^{th}-order finite difference CFD code is chosen to resolve the modes of interest even at a limited grid resolution [7].

In the following study, validations between DNS and LST simulations of the 2D modes are discussed. They are shown, based on boundary-layer profiles examined by Seitz [8] in comparison with results from the LST. Temporal approaches as well as spatial simulations by DNS are compared with LST data containing the growth rates and the perturbation profiles. Furthermore, physical questions like influences of steps at realistic laminar airfoils on TS-wave amplification will be addressed.

For manufacturing reasons, a realistic wing is never expected as an ideal perturbation-free surface, so influences of surface imperfections must be taken into account for the laminar-wing design with or without suction. Influences of these surface bumps or steps by rivets or joints of wing-panels must be predictable within the design-loop by quick generic computational tools, due to their essential influence on the position of transition and consequently the friction-drag. For this reason, detailed analysis of the physics behind these influences of surface imperfections on boundary-layer stability is an important task for future laminar aircraft configurations.

Within this study, perturbations of the laminar boundary-layer, generated by a forward facing step (see Fig. 2) will be investigated numerically in detail with respect to transitional two-dimensional boundary-layer modes such as Tollmien-Schlichting (TS) waves. The behavior of these instabilities will be predicted by Direct Numerical Simulations (DNS) of their transitional growth in the laminar boundary-layer over the step, including non-linear effects in the boundary-layer up- and downstream of the step. The application of standard methods like the Linear Stability Theory (LST) is generally not possible in this region without additional assumptions, since directly at the step a singular behavior of the flow is observed. In contrast, the direct simulation of TS-waves provides a high resolution of the phenomena behind the step, including non-linear viscous effects. It is only limited by the two-dimensional approach of the x-y grid.

A destabilizing effect of the step was shown in different studies [9], by investigating the growth of BL-instabilities behind steps of different physical dimensions. This additional amplification of TS-waves in plane BL will finally result in an earlier transition downstream of the step region.

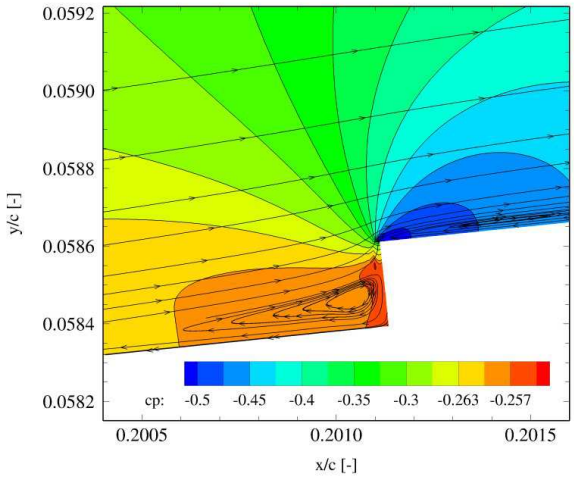

Figure 2: Pressure (c_p) distribution at a forward-facing step including time-averaged streamlines from DNS-simulations on the refined partial grid

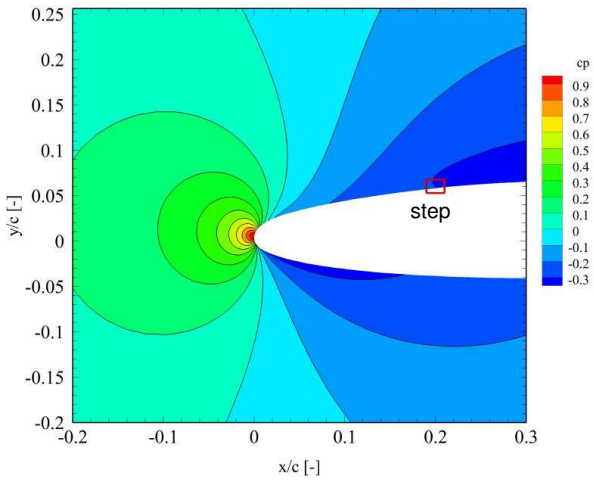

Figure 3: Pressure distribution from the 4^{th}-order finite difference scheme on the fine grid (detail)

For comparison with the numerical flow-calculations, within the LUFO-DLR project ATLATUS a wind tunnel model was manufactured with a pressure distribution in the center-line, similar to a realistic laminar wing-profile of a commercial airplane (see Fig. 3). This configuration (see Fig. 1) was measured in detail in the DNW-NWB at the DLR-Braunschweig by various methods, i.e. infrared thermography for receiving the transition-location. For this purpose, the laminar-airfoil contains an adjustable step in the leading-edge region at 20% wing-chord.

Time-resolved numerical calculations were carried out by the structured Navier-Stokes solver FLOWer, using a 4^{th}-order finite difference (FD) scheme in implicit formulation, stabilized by high-order Pade-filters as implemented by S. Enk [7]. While the standard-version of this code provides second-order finite volume formulations for highly accurate and robust steady RANS-simulations [10], unsteady direct simulations of Boundary-layer-modes and their growth can be predicted by the high-order approach. This method was widely validated in former studies for different flow-conditions (see [1, 2]). In the following section, the second-order scheme is used for steady RANS-results of the complete wing-profile on sufficiently resolved grids for the base-flow under various angles of attack. These grids are nevertheless not sufficient for a suitable resolution of transitional modes. The TS-modes are calculated on even finer grids by FD. Since no cross-flow components are apparent in the boundary-layer of the wind tunnel model, two-dimensional simulations are sufficient as long as the breakdown to turbulence does not appear and nonlinear effects can be omitted.

To reduce computational costs, the calculation region of the DNS is restricted to a section in the periphery of the step, using an extensively refined mesh to resolve TS-waves with at least 40 cells per wavelength. For the gradients near the step, the grid is especially improved directly at the corner of the step. The steady flow-field of the wing-profile is calculated by the finite-volume scheme, including a predicted transition location and the k-ω–SST RANS-model for the turbulent part of the BL. The predicted flow-field allows a direct comparison to the data of the wind tunnel experiment in the DNW-NWB. The results of the RANS-calculations were used as a start-up for the direct simulations and interpolated on the refined grid. The boundary-layer at the inflow was kept fixed along the unsteady simulation, since the perturbations are expected to act as small superpositions.

Numerically, the inflow BL of the region near the step is almost free of perturbations and needs an injection of defined instability-modes. For this reason, a mono-frequent disturbance with a given amplitude in the wall-normal velocity-component is added at the inflow-boundary of the refined grid and the resulting amplified waves are investigated behind the step in comparison with the predicted instability scenario. Based on this results a validation of empirical transition-criteria, including the step dimension additionally to the standard LST-approach, will be possible.

2. NUMERICAL SIMULATION TOOLS

2.1. Direct numerical simulation

The direct numerical simulations are carried out by a 4^{th}-order compact finite difference version of the DLR Flower-code implemented by Enk [7]. While the basic FLOWer-code solves the compressible Reynolds-averaged Navier-Stokes equations on block-structured grids with second-order finite volume techniques, the high-order version uses 4^{th}-order central differencing based on a standard compact approach, including the complete infrastructure of the code. High-order compact filters are applied at the end of each time step.

2.2. Basic equations

The basic equations and numerical schemes of the compressible high-order FLOWer-code will be described in the following [7]. Generally a 4^{th}-order central differencing scheme based on a standard compact approach was used for the DNS. High-order compact filters, that are applied at the end of each time step and sponge-zone boundary conditions are optional to reduce reflections. For the present work a 6^{th} order filter and the standard conservative form of the Euler terms is chosen. Time advancement is applied by a five-step second-order Runge-Kutta method. The solved equations for a perfect gas with density ρ, velocity components u_i, pressure p and internal energy e, are written in conservation law form as

$$\frac{\partial \rho}{\partial t} + \frac{\partial \rho u_j}{\partial x_j} = 0 \tag{1}$$

$$\frac{\partial \rho u_i}{\partial t} + \frac{\partial \rho u_i u_j}{\partial x_j} + \frac{\partial p}{\partial x_i} = \frac{\partial \tau_{ij}}{\partial x_j} + f_i \tag{2}$$

$$\frac{\partial \rho E}{\partial t} + \frac{\partial (\rho E + p) u_i}{\partial x_i} = -\frac{\partial q_i}{\partial x_i} + \frac{\partial u_i \tau_{ij}}{\partial x_j} + g, \tag{3}$$

where $E = e + u_i u_i / 2$. Especially for a temporal TS-wave simulation, forcing terms f_i and g are included in the right hand side of the equations, such that a specified parallel base flow $\overline{\rho}(y), \overline{u}_i(y), \overline{E}(y)$ is time independent for comparisons of DNS results with the temporal LST data. In practice these terms are

evaluated numerically within the code by computing and storing the initial residual. For spacial simulations of TS waves, no source terms are necessary, since the boundary-layer will grow naturally, in these cases f_i and g are always zero. The equations are closed with the perfect gas law and the constitutive relations for q_i and τ_{ij} [7]. This approach is used without modifications as a basis for all calculations on different grids.

2.3. Linear stability theory

For the following investigations, the local linear approach is applied which is a subset of the non-local stability equations. The Lilo-code [11, 12], which is a spatial linear stability solver, is a development of Airbus and can be used for linear stability analysis as well as parabolized stability equations.

The stability equations are derived from the conservation of mass, momentum and energy, governing the flow of a viscous, compressible, ideal gas, formulated in primitive variables. All flow and material quantities are decomposed into a steady laminar base flow $\bar{q}$ and an unsteady disturbance flow $\tilde{q}$.

$$q(x, y, z, t) = \bar{q}(x, y) + \tilde{q}(x, y, z, t) \tag{4}$$

The perturbation $\tilde{q}$ is represented as a harmonic wave

$$\tilde{q}(x, y, z, t) = \hat{q}(x, y) \exp[i(\alpha x + \beta z - \omega t)] \tag{5}$$

with the complex valued amplitude function $\hat{q}$. Since LILO is a temporal code, the frequency ω is a complex value while the wave numbers α and β are real quantities. The growth rate is defined by ω_i, which is the imaginary part of the complex frequency. For validations by TS-waves the chosen DNS approach is inherently temporal, so a direct comparison between DNS and LST is possible. LILO is validated by several test cases against published results, including DNS, PSE (parabolized stability equations), multiple scales methods and LST. For the ATLATUS wind tunnel campaign, transition lines of the smooth airfoil without step were calculated very successfully in the design phase by this tool in combination with the BL-solver COCO from the same toolbox (see Fig. 4).

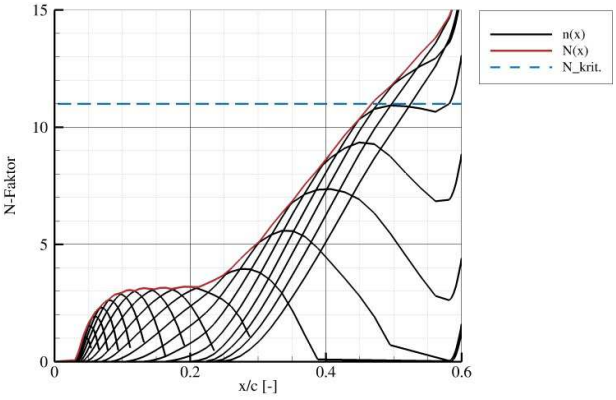

Figure 4: Example for n-Factor curves of the ATLATUS-airfoil along the chord x/c for the wing-profile design

3. GRIDS AND FLOW-CONDITIONS

3.1. CFD-grids

All simulations were carried out on structured 2D-grids around the laminar wind tunnel airfoil (Fig. 5). A C-topology of the grid was chosen by using a hyperbolic grid-generator. Refinement of the global grid with 35200 elements was introduced in the wake and in regions with strong pressure-gradients, such as the forward-facing step at 20% chord. For all steady RANS-simulations, only grids around the entire wing-profile are in use, while DNS of the unsteady behavior of TS-instabilities is always calculated on refined mesh-parts around the step. This cut-out section with about 200000 elements is shown in Fig. 6. Up to 396 zones where chosen for the parallel calculations. Such a high domain-decomposition was necessary, due to the costly unsteady simulations of the traveling TS-modes in the boundary layer. Near the step, a high equidistant resolution in streamwise-direction was chosen,

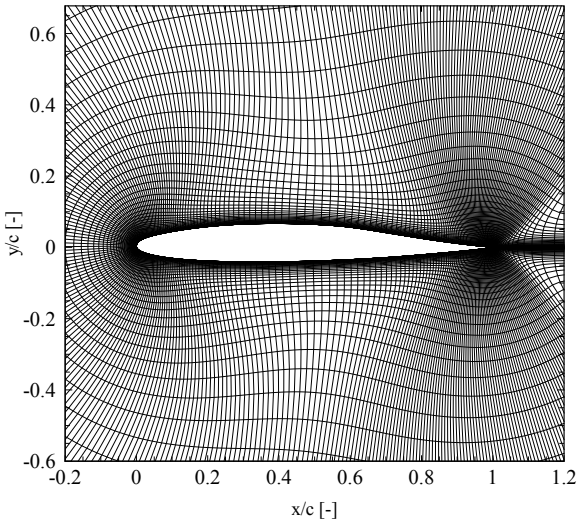

Figure 5: CFD grid for RANS-simulations without step around the profile (scaled by the chord $c = 2,75m$)

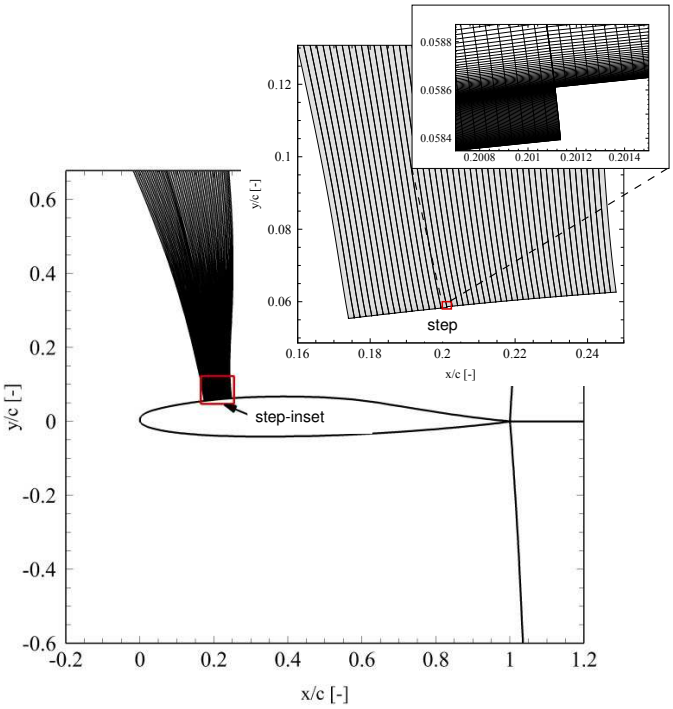

Figure 6: Overview of the extracted grid-part in the step-region for DNS-calculations, scaled by the profile depth $c = 2,75m$

which was well-adapted for the study of TS-growth [1]. For this purpose an additional script interpolated additional cells in streamwise direction, by keeping the shape of the original profile. The wall-normal cell-spacing was kept from the steady simulation, since former validation-studies have shown a sufficient resolution for the TS-waves in this region. The use of an automated refinement allowed free choice of DNS-cutouts, blockings and refinement-parameters near the step and resulted in a quick grid-generation for parameter studies. The temporal calculations of the laminar-airfoil use a prescribed inflow boundary condition with an approximated unsteady perturbation-profile and a simple extrapolation-condition at outflow in wall-normal direction. The perturbation-profile is harmonically varied in time, to introduce a well-defined amplified mode into the boundary-layer. No-slip walls at adiabatic wall temperature are applied. At the farfield-boundaries, characteristic conditions, including a standard sponge-layer are used. The initial steady solution for generic boundary-layers and for inflow conditions is obtained from the RANS solution of the entire grid and interpolated onto the DNS-region.

3.2. Inflow-conditions

As a computation base for the local DNS around the step of the ATLATUS-model, the calculated pressure distribution is compared with the DNW-NWB data (see section 4.2). For this study, only one set of conditions is chosen, detailed comparisons

Table 1: Reference-parameter for the RANS and DNS-simulations

U_∞	$80\ \frac{m}{s}$
M_∞	$0,2292$
Re_c	13769040
α	$-0.3\,^\circ$
T_∞	$303,15\ K$
p_∞	$101325\ Pa$
Pr	$0,72$

are found in [13]. In accordance with the DNW-NWB conditions, inflow velocities were set in the far-field at $u_\infty = 80\frac{m}{s}$ and an angle of attack α of $-0.3\,^\circ$ which is the design-angle. These steady calculations were carried out for the profile without step, except some preliminary tests of the numerical scheme and base-simulations for the DNS. Due to the airfoil-design in the wind tunnel in comparison with the CFD-grid, an angle-correction was necessary for direct comparisons, this difference-angle is already included in the following descriptions of all test-cases. All parameters for the following RANS-results are specified in Tab. 1. For additional temporal validation test-cases a Mach-number $M_\infty = 0.204$, a Reynolds number based on the displacement thickness of $\mathrm{Re}_{\delta 1} = 2900$, corresponding to flight No. 8, Measuring point 13 at $x/c = 0.34$ from the flight-experiments of Seitz [8], is considered. The wall-normal co-ordinate as well as all other quantities derived from spatial co-ordinates are normalized by the displacement thickness. This temporal DNS of the instabilities is initialized by an artificial disturbance at $t = 0$ which is given by a decaying v-velocity component with a harmonic part in streamwise direction. For the perturbation-profile, a general analytic function in the wall-normal velocity-component that mimics the perturbation-profile of a TS wave by a quadratic exponential profile. This add-on function in space is given at the initial time-step by:

$$v' = v_{amp} \cdot exp(-(y - y_{max})^2) \cdot sin(\alpha x) \qquad (6)$$

which is a typical approximation for a TS wave in space it will decay during the first few thousand time steps while the amplified eigenfunction at the boundary-layer will develop. Here v_{amp} is the amplitude while y_{max} is the respective wall-normal location of the maximum in the profile.

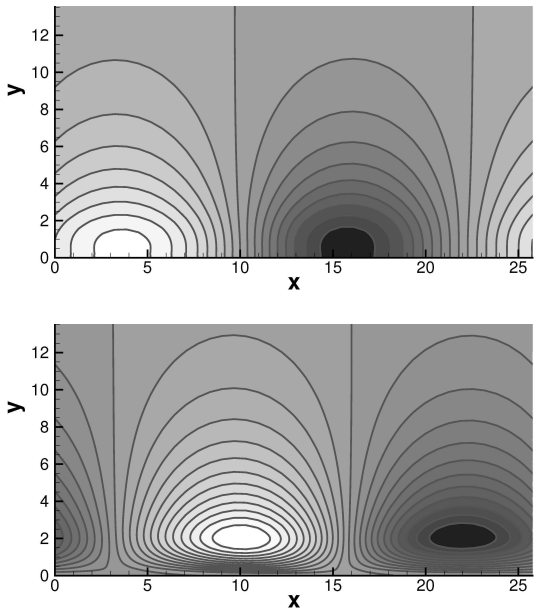

Figure 7: Development of TS waves in a subsonic boundary-layer at $M_\infty = 0.204$, $Re_{\delta 1} = 2900$. Top: pressure contours, bottom: contours of normal velocity

4. NUMERICAL RESULTS

4.1. Validation of the DNS simulation tool by comparison with flight-test data

As a first step the abilities of the code in predicting growth rates of TS waves by a temporal approach are tested. Comparisons are carried out with flight-data from Seitz [8] (see 3.2). Pressure and velocity contours for temporal DNS calculations of TS waves are shown in Fig. 7 for the boundary-layer flow at $M_\infty = 0.204$, $\mathrm{Re}_{\delta 1} = 2900$ to provide an overview of the mode shape in terms of these quantities. From these simulations, perturbation-profiles and amplification rates are extracted as shown in Fig. 8 in comparison with LST data. As shown in (Fig. 8b). Very good agreement is achieved for the eigenfunctions as well as for the amplification rates [1], which deviate by less than 0.4%. Therefore, the high-order approach for the direct simulation of TS-modes is well justified by these calculations.

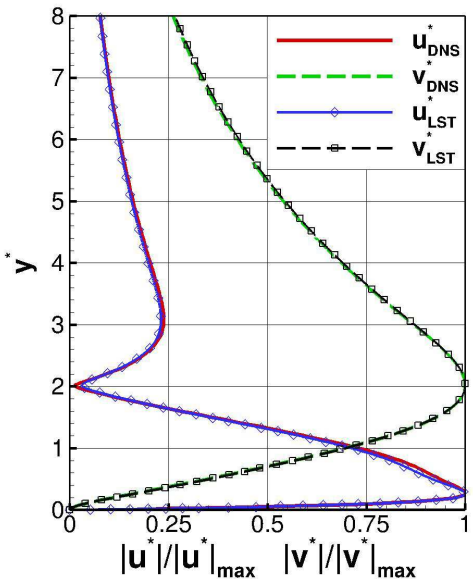

Figure 8: DNS and LST of a TS wave at $M = 0.204$, $Re_{\delta 1} = 2900$, $U_\infty = 85.4m/s$, (a) comparison of eigenfunction shape. (b) Direct numerical simulation of perturbation-amplitude (symbols) and linear fit of the growth rate (solid line)

4.2. Steady RANS-results, including LST

In the following section, the pressure-distribution of the 2D RANS-result of the laminar-airfoil without step are compared with DNW-NWB measurements. Furthermore, comparisons of different numerical approaches, used for RANS or DNS predictions, are cross-checked for the geometry with forward-facing step.

in Fig. 9, the pressure-coefficients from simulation and experiment are compared for the conditions from Tab. 1. Due to differences in the inflow definition and especially non-planar effects of the model flow-field in the center-cut, a shift in the pressure distribution is visible by two scales, used in the ordinates. This offset in c_p is not a severe concern for the following calculations, since the main influence on TS-wave growth is the pressure-gradient in the area of interest, which is in good agreement near the step-position. Further downstream and on the leeward side, additional differences in the pressure distribution are visible, they are of minor interest, since in these regions the breakdown to turbulence

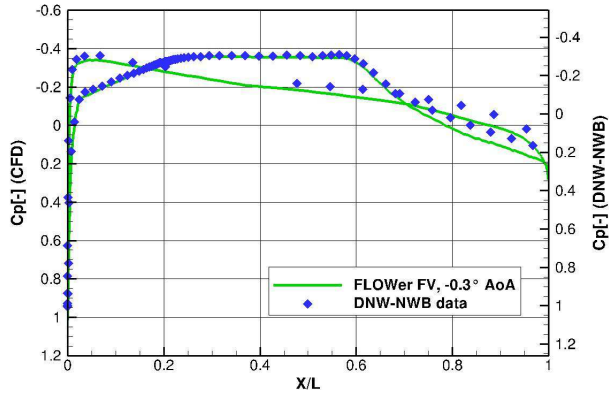

Figure 9: Pressure distribution for geometry without step from RANS-results in comparison with wind tunnel data

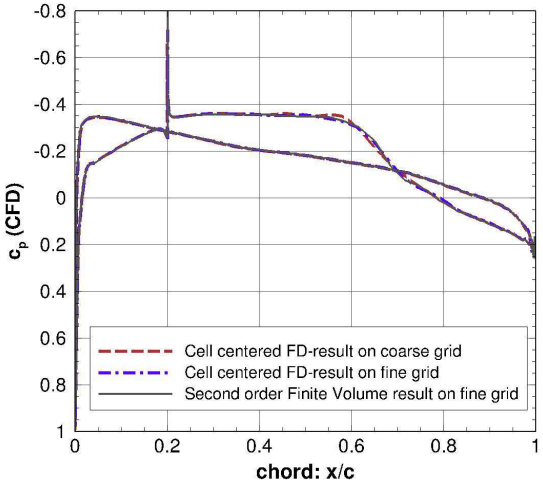

Figure 10: Comparison of the pressure distribution including step. RANS calculations from different numerical schemes with step along the laminar profile at $\alpha = -0.3\,^{\circ}$

is already apparent and would make TS-wave simulations pointless.

To evaluate the RANS-results for the wing-profile with step and to cross-validate second-order finite-volume predictions with the implicit finite-difference approach, steady calculations were carried out on grids of different resolution around the entire airfoil-cut. The results for both numerical schemes are nearly identical, as shown in Fig. 10. In the region of the step, a suction peak is generated and equally well predicted by both schemes. The dominating influence of the step on the surface pressure decreases further downstream, as demonstrated in the diagram. Very small deviations in the range of $\Delta c_p \approx 0,002$ appear near the step, since higher-order schemes have the capability to resolve gradients near the singularity, even on the comparatively coarse grid resolution.

4.3. Spacial DNS-simulation of TS-waves behind the step

With the validated technique of direct TS-mode calculation, the development of TS-waves over the forward facing step with re-circulating flow is investigated by the implicit FD-approach. The capabilities of the code have been demonstrated as well in former studies [1] by generic step-geometries. Flow-conditions are taken from Tab. 1 for the standard wind-tunnel investigations. The steady base-profile at inflow was extracted from the Navier-Stokes simulations of the steady boundary-layer and interpolated onto the refined partial grid. Approximations

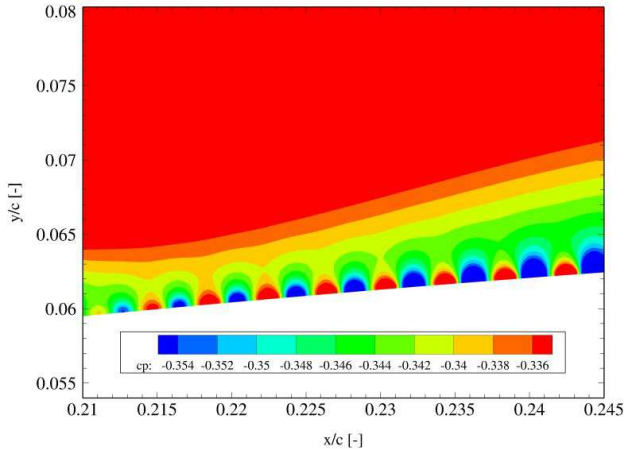

Figure 11: TS-wave behind step: Perturbation pressure of the transitional mode from DNS on the refined grid (base flow with superimposed instability contours)

of TS-mode perturbation-function at a small amplitude A_0 of $0,2\%$ wall-normal velocity are added to the steady inflow velocity-profile. This amplitude was chosen in order to stay safely in the linear regime of the perturbation, everywhere in the airfoil boundary-layer of the extracted DNS-part. From the prescribed perturbation, the boundary layer upstream of the step will filter the final TS-wave, which will be investigated behind the step.

The resulting contours of the perturbation pressure along the boundary-layer are shown in Fig. 11 for the perturbed flow in a selected region to demon-

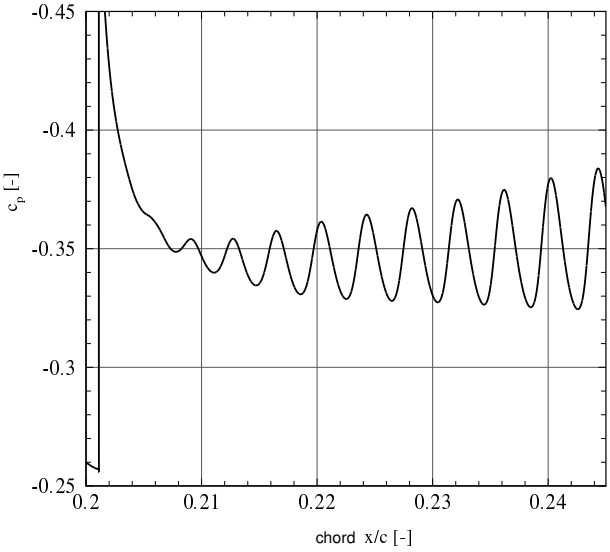

Figure 12: Surface-pressure distribution from DNS on the grid-detail on the upper part of the profile behind the step

strate the mechanism of instability generation. In this region, the perturbations are visibly amplified, as shown in the subsequent diagram of the surface pressure, where the singularity of the step appears at at $x/c = 0.2$, while the unstable mode is growing from $x/c = 0.21$ on (Fig. 12).

5. CONCLUSIONS

The goal of this work was the direct simulation of local instabilities behind a forward-facing step on a laminar airfoil in the DNW-NWB wind tunnel. For this reason a well-validated high-order numerical scheme was chosen for direct simulations of the transition-modes, which has been shown to be well-suited for growth rate-predictions of BL instabilities.

Steady 2D RANS-simulations with a second-order finite volume scheme and a two-equation RANS-model as well as DNS on the laminar airfoil-geometry have shown good agreements with wind tunnel data in comparison with pressure distributions and TS-wave growth. In a next step, different numerical approaches, like FV and high-order implicit FD, are applied for steady airfoil-calculations including forward facing steps. In comparison they have shown very good agreement between different approaches on coarse- or fine grids.

Grids for the direct simulation of TS-waves, generated as strongly refined cut-outs of the original airfoil-contour, were used to interpolate the steady RANS-results from the preliminary calculations onto these regions to generate a base-flow for the direct TS-wave predictions.

By preliminary validation-studies, using BL-data from a free-flight experiment, the capabilities of the numerical scheme in simulating growth rates of TS-modes were demonstrated in good agreement.

For the DNS calculations, unsteady mono-frequent velocity-perturbations were added at inflow-boundaries and a realistic behavior of TS-instabilities was found behind the step by using the high-order Navier-Stokes solver. In agreement with LST-predictions, amplified TS-waves are investigated downstream of the step. As a result, the development of growing unstable instability-modes was demonstrated successfully downstream of the step-region. The process chain, reaching from the steady simulation of the background flow-field to the implementation of temporal perturbations at the inflow plane, has shown the capabilities of the presented approach. Once again the applicability of the chosen local DNS of TS-instabilities as a supporting technique for LST-design is well confirmed.

Considering these results, growth rates of TS-waves can be compared with different LST-predictions including empirical extensions in the step-region within future studies.

ACKNOWLEDGMENTS

The authors acknowledge the DNW-NWB for providing the wind tunnel data from the ATLATUS-campaign in 2015. We would like to thank Dominic Gloß for valuable discussions. A major part of the study was carried out under the scope of the German Federal research programme for aeronautics LuFo-IV.

REFERENCES

1. Lüdeke, H., Wartemann, V. & Seitz, A. (2010) Direct Numerical Simulation of Tollmien Schlichting Waves to Support Linear Stability Analysis. Notes on Numerical Fluid Mechanics and Multidisciplinary Design **121,** pp. 227–234.
2. Backhaus, K. (2014) Direkte numerische Simulation der Anfachungsraten von Tollmien-Schlichting-Wellen. Bachelorarbeit Institut für Strömungsmechanik, Technical University Braunschweig.
3. Horstmann, K. (2014) Flügelentwurf. In: Handbuch der Luftfahrzeugtechnik (Eds. Rossow, C.-C., Wolf, K. & Horst, P.), pp. 173–184.
4. Joslin, R.D. (1998) Overview of laminar flow control. NASA/TP-1998-208705.
5. Tollmien, W. (1935) Ein allgemeines Kriterium der Instabilität laminarer Geschwindigkeitsverteilungen. Nachr. Ges. Wiss. Göttingen, Math. Phys. Klasse, Fachgruppe I, pp. 79–114.
6. Schlichting, H. (1935) Amplitudenverteilung und Energiebilanz der kleinen Störungen bei der Plattenströmung. Nachr. Ges. Wiss. Göttingen, Math. Phys. Klasse, Fachgruppe I, pp. 47–78.
7. Enk, S. (2007) Ein Verfahren höherer Ordnung in FLOWer für LES. DLR IB-124-2007/8 **57**.
8. Seitz A. (2007) Freiflug-Experimente zum Übergang laminar-turbulent in einer Tragflügelgrenzschicht. Dissertation Technical University Braunschweig. Published as DLR-Forschungsbericht FB-2007-01.

9. Perraud, J., Arnal, D., Seraudie, A. & Tran, D. (2004)
Laminar-turbulent transition on aerodynamic surfaces with imperfections.
RTO-AVT-111, Prag ONERA, pp. 1–13.

10. Kroll, N., Rossow, C.C., Schwamborn, D., Becker, K., & Heller, K. (2002)
Megaflow - a Numerical Flow Simulation Tool for Transport Aircraft Design.
ICAS 2002 Congress.

11. Schrauf, G., Horstmann, K.H. (2001)
Linear Stability Applied to Natural and Hybrid Laminar Flow.
Notes on Num. Fluid Mechanics **76,** pp. 157–163.

12. Schrauf, G. (2003)
Industrial view on transition prediction.
(Eds. Wagner, S., Kloker, M. & Rist, U.)
Recent results in laminar-turbulent transition. Selected numerical and experimental contributions from the DFG priority programme "Transition" in Germany.
In: Numerical Notes of Fluid Mechanics and Multidisciplinary Design (NNFM) **86,** pp. 111-122.

13. Backhaus, K. (2015)
Direkte numerische Simulation der Anfachungsraten von Tollmien-Schlichting-Wellen über Stufen mit einem Finite-Differenzen-Verfahren höherer Ordnung.
Studienarbeit Institut für Aerodynamik und Strömungstechnik, DLR Braunschweig.